13th World Conference on Earthquake Engineering
Vancouver, B.C., Canada
August 1-6, 2004
Paper No. 2375

CHARACTERISTICS OF LIQUEFIED SILTY SANDS FROM MEIZOSEISMAL REGION OF SHILLONG PLATEAU, ASSAM AND BHUJ IN INDIA

T.G.SITHARAM[1], L.GOVINDARAJU[2], B.V.RAVISHANKAR[2] and B.R.SRINIVASA MURTHY[3]

SUMMARY

This paper describes the results of an experimental study on the undrained behavior of liquefied silty sands collected from the two regions of earthquake affected areas namely Beltaghat in Assam state and Bhuj in Gujarat State in India. In the present study both static and dynamic testing of soil was carried out by employing a servo-controlled electro hydraulic closed loop test system. Stress - controlled cyclic triaxial undrained shear tests were carried out on soil specimens from Bhuj area and Strain – controlled cyclic triaxial undrained shear tests were carried out on soil specimens from Assam area. In all the tests a sinusoidal loading with a frequency of 1Hz was maintained. The potential for liquefaction of both soils was evaluated for the range of relative densities from 20% to 75% under an effective confining pressure of 100 kPa. Also, undrained triaxial shear tests under monotonic loading were conducted on soil specimens from Bhuj area to establish steady-state and quasi-steady state lines for the range of relative densities 20% to 80% and confining pressures 25 kPa to 450 kPa to estimate the residual strength of liquefied silty sands. By examining the laboratory test data, the liquefied silty sand from Bhuj consisting of appreciable amount of fines showed the residual strength to be a function of effective confining pressure and void ratio. Further, cyclic triaxial test results clearly explain that there is a consistent relationship between cyclic shear strain and pore pressure generation in silty sand.

INTRODUCTION

Many earthquake induced ground failures have occurred in silty sands. Recent new findings, indicating the importance of silt content, have potential implications for liquefaction of level ground, hydraulic fills, and earth dams, in which the silt content may be quite high (Yamamuro and Lade) [3]. The occurrence of great earthquake (M = 8.7) in Assam, India during 1897 in the shillong plateau succeeded by three great earthquakes (1905, 1934 and 1950) in the adjoining Himalayan frontal arc, indicates the vulnerability of the Shillong Plateau to large earthquakes and intense liquefaction of silty sands in the river bed profiles (Sukhija et al.,) [5]. The seismic events resulted in severe liquefaction followed by flooding. The liquefaction observed was highly pervasive and intense causing many vents from which water carrying sand ejected to a height of about 3 to 5 m (called as sand dykes). Several sand dykes were observed near the Krishnai River, which is the north flowing tributary of the Brahmaputra River. Figure 1shows the location map of Assam and Beltaghat site and figure 2 shows the geologic cross-section along the Krishnai River bank where the earthquakes have left their signatures at Beltaghat interms of multiple sand

1 Associate Professor, Department of Civil Engineering, Indian Institute of Science, Bangalore (INDIA)
2 Research Scholars, Department of Civil Engineering, Indian Institute of Science, Bangalore (INDIA)
3 Professor, Department of Civil Engineering, Indian Institute of Science, Bangalore (INDIA)

dykes. Also the Bhuj earthquake that struck the Kutch area in Gujarat at 8.46 AM (IST) on January 26, 2001 with a magnitude of Mw = 7.7 was the most damaging earthquake in India in the last 50 years. The epicenter of the quake was located at 23.4° N, 70.28^0 E at a depth of 25 km, which is to the north of Bacchau town (Srivastava) [4]. Figure 3 shows the location of epicenter of the earthquake. In most of the locations of the affected area, water and sand vented through ground cracks. Several sand blow craters were developed and a crater of 3m wide near Lodai (Figure 4) continued to spout water for three weeks after the earthquake. These observations bring home the severity of the earthquakes those struck these regions and left their signatures in terms of these liquefaction evidences. The post-earthquake behavior of soil and, consequently the stability of structures founded on liquefied soil, depend on the post-liquefaction shear strength of soil. The strength of soils mobilized at the quasi-steady state has important implications for engineering practice (Ishihara) [2].

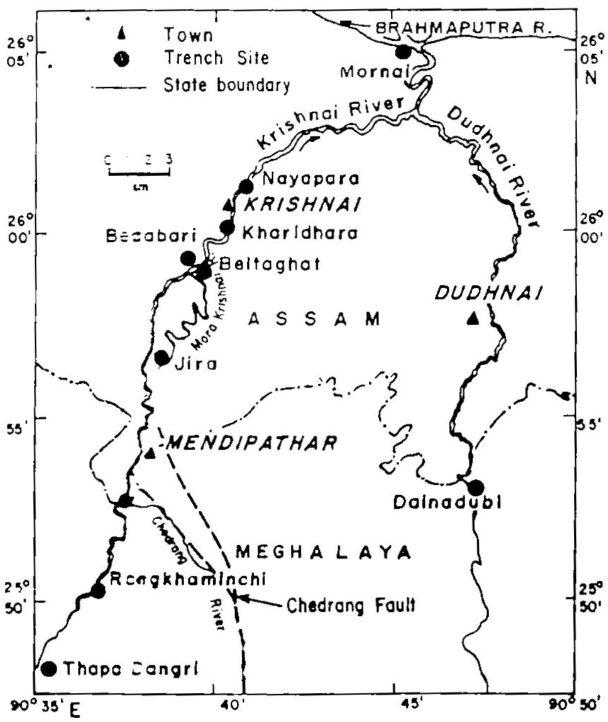

Fig.1 Location map of Assam and Beltaghat (Sukhija et al. 1999)

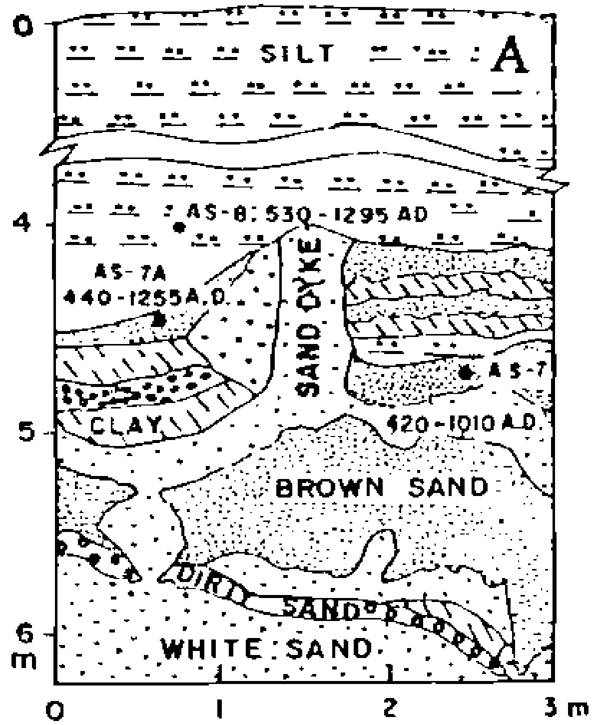

Fig.2 Earthquake induced multiple sand dykes at Beltaghat (Sukhija et al. 1999)

1 Associate Professor, Department of Civil Engineering, Indian Institute of Science, Bangalore (INDIA)
2 Research Scholars, Department of Civil Engineering, Indian Institute of Science, Bangalore (INDIA)
3 Professor, Department of Civil Engineering, Indian Institute of Science, Bangalore (INDIA)

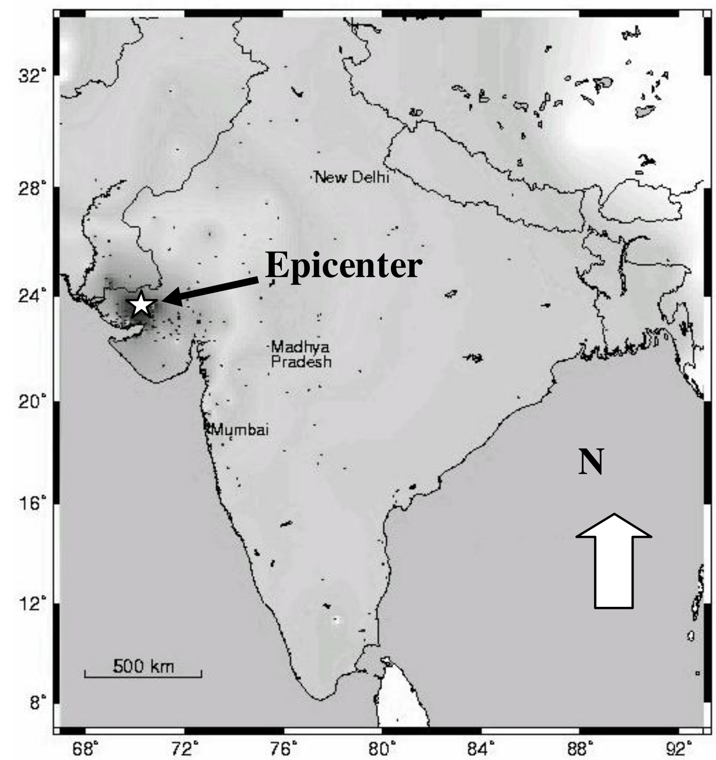

Fig.3 Location map of epicenter of Bhuj earthquake in 2001

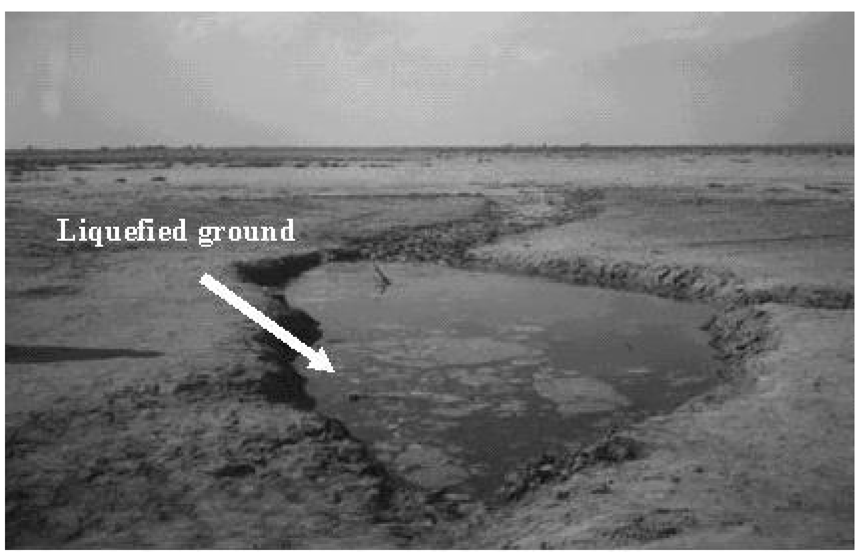

Fig.4 Extensive liquefaction near Lodai

1 Associate Professor, Department of Civil Engineering, Indian Institute of Science, Bangalore (INDIA)
2 Research Scholars, Department of Civil Engineering, Indian Institute of Science, Bangalore (INDIA)
3 Professor, Department of Civil Engineering, Indian Institute of Science, Bangalore (INDIA)

EXPERIMENTAL INVESTIGATION

Materials

At Beltaghat site, a very prominent sand dyke rising from 6 m depth was observed. The height of the sand dyke was about 2 m and its width was about 30 cm (Fig. 2). Soil samples were collected from this dyke. Also, liquefied and oozed out soil sample was collected from the ground surface from the location very close to the epicenter of the Bhuj earthquake (Fig.3). Figure 5 shows the particle size distribution and Table 1 gives the summary of the index properties of both soil samples.

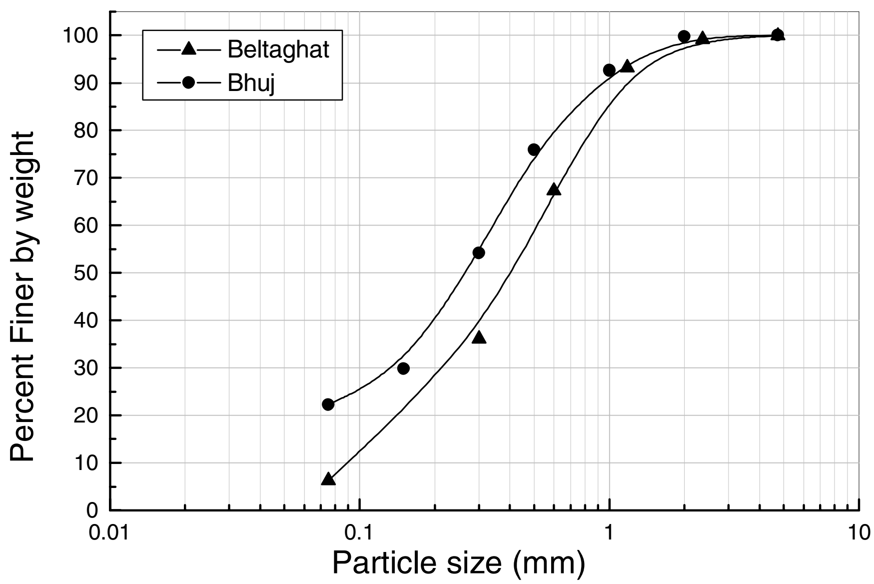

Fig. 5 Grain size distribution of liquefied soils from Beltaghat and Bhuj sites

Table 1 Index properties of soil samples

Index Property	Beltaghat Location	Bhuj Location
Specific Gravity	2.66	2.67
Medium sand (%)	48.8	35.0
Fine Sand (%)	45.0	43.0
Fines content (%)	6.2	22.0
Maximum void ratio (e_{max})	0.91	0.68
Minimum void ratio (e_{min})	0.53	0.42

Cyclic Triaxial Testing Equipment

A Computerized Automated Triaxial Testing System with six sensors, including a load cell to monitor the axial load, an LVDT to measure the vertical displacements, four transducers to detect the chamber pressure, pore water pressure, volume change and lateral deformation was used in this study. The triaxial

1 Associate Professor, Department of Civil Engineering, Indian Institute of Science, Bangalore (INDIA)
2 Research Scholars, Department of Civil Engineering, Indian Institute of Science, Bangalore (INDIA)
3 Professor, Department of Civil Engineering, Indian Institute of Science, Bangalore (INDIA)

cell is built with low friction piston rod seal to which a servo-controlled submersible load cell of capacity 10 kN is fitted. The loading system consists of a load frame and hydraulic actuator capable of performing strain-controlled as well as stress-controlled tests with a frequency range of 0.01 Hz to 10 Hz employing built in sine, triangular and square waveforms or any other random loading waveforms by means of external input. The specimens of size 38mm, 50mm, 75mm and 100mm diameter can be tested with confining stresses up to 1000 kPa. The conditioned output from the sensors is received by process interface, which forms the communication link between the computer and the loading system.

Sample Preparation

Soil specimens of size 50 mm diameter and 100 mm in height were prepared using pouring technique (ASTM Designation: D 5311-92)[1]. The sand was initially saturated in a container. Saturated sand was poured through water into the water-filled forming mould and then densified to the required density by giving gentle vibrations to the mould. Each specimen was prepared at different target relative densities (RD). The specimens were then saturated with deaired water using backpressure saturation. The backpressure was increased gradually while maintaining the effective confining pressure at 15 to 20 kPa. This process was continued until the pore pressure parameter B (= $\Delta u/\Delta\sigma_c$, Δu = change in specimen pore pressure, $\Delta\sigma_c$ = change in confining pressure) exceeded 0.95. Following saturation, the sand specimens were consolidated to an effective isotropic consolidation stress of 100 kPa.

Cyclic Loading and Data Acquisition

Soil samples form Beltaghat prepared at three different relative densities 20%, 50% and 75% were subjected to cyclic loading using strain-controlled method. Tests were carried out on soil samples at constant shear strain amplitude in the range of 0.14% to 0.55%. Figures 6 and 7 show the typical test results of the Beltaghat soil sample. Stress-controlled cyclic triaxial tests were conducted on Bhuj soil samples at a constant Cyclic Stress Ratio (CSR = $\sigma_{dc}/2\sigma_c^{'}$, σ_{dc} = cyclic stress, $\sigma_c^{'}$ = effective confining pressure) of varying magnitudes. Cyclic Stress Ratios of 0.03, 0.08 & 0.14 for specimen with relative density 51%, 0.07, 0.082 & 0.132 for specimen with relative density 60% and 0.07, 0.08, 0.14 & 0.18 for specimen with relative density 69.7% were used. Figures 8 and 9 show the typical test results of Bhuj soil. In both strain-controlled and stress –controlled tests, a harmonic loading was applied using sine wave with a frequency of 1Hz. Axial deformation, cell pressure, cyclic load and sample pore water pressure were monitored using a built-in data acquisition system.

Figure 6 shows a typical plot of a strain-controlled cyclic triaxial test on Beltaghat soil sample prepared at a relative density of 50% and subjected to a constant amplitude of shear strain (γ = 0.51%). It is evident from the figure 6 that as the number of strain cycles increase, the excess pore water pressures build up. This progressive build up of excess pore water pressure cause a substantial reduction in the effective stress and finally the effective stresses reduce to zero when the pore pressure ratio is equal to one. In this case, the soil liquefies in 14 cycles of shear strain application. Figure 7 illustrate the liquefaction resistance curves for the Beltaghat soil sample. It can be observed from the figure 7 that as the magnitude of shear strain increases, the number of strain cycles required to initiate liquefaction reduces. This clearly indicates that the magnitude of shear strain govern the rate of pore pressure build up during cyclic loading. Also, as observed from the figure 7 the resistance for liquefaction of the soil increases as the relative density of the soil increases.

Figure 8 shows a typical plot of variation of effective mean stress (p') with the deviator stress (q) for the Bhuj soil at a relative density of 51% using stress-controlled technique. Here the soil liquefies in five cycles of uniform load applications at a cyclic stress ratio of 0.14. The data shown in the plot is from the second cycle. Figure 9 represent the cyclic resistance curves of the silty sand tested at varying relative

1 Associate Professor, Department of Civil Engineering, Indian Institute of Science, Bangalore (INDIA)
2 Research Scholars, Department of Civil Engineering, Indian Institute of Science, Bangalore (INDIA)
3 Professor, Department of Civil Engineering, Indian Institute of Science, Bangalore (INDIA)

densities (RD). It is clear from the Fig. 9 that the cyclic strength of silty sand increases as the relative density of the soil increases. The cyclic strength of silty sand (specified in terms of the magnitude of cyclic stress ratio required to produce 5% double amplitude axial strain in 20 cycles of uniform load application) can be read as 0.082, 0.1 and 0.182 for relative densities 51%, 60% and 69.7% respectively

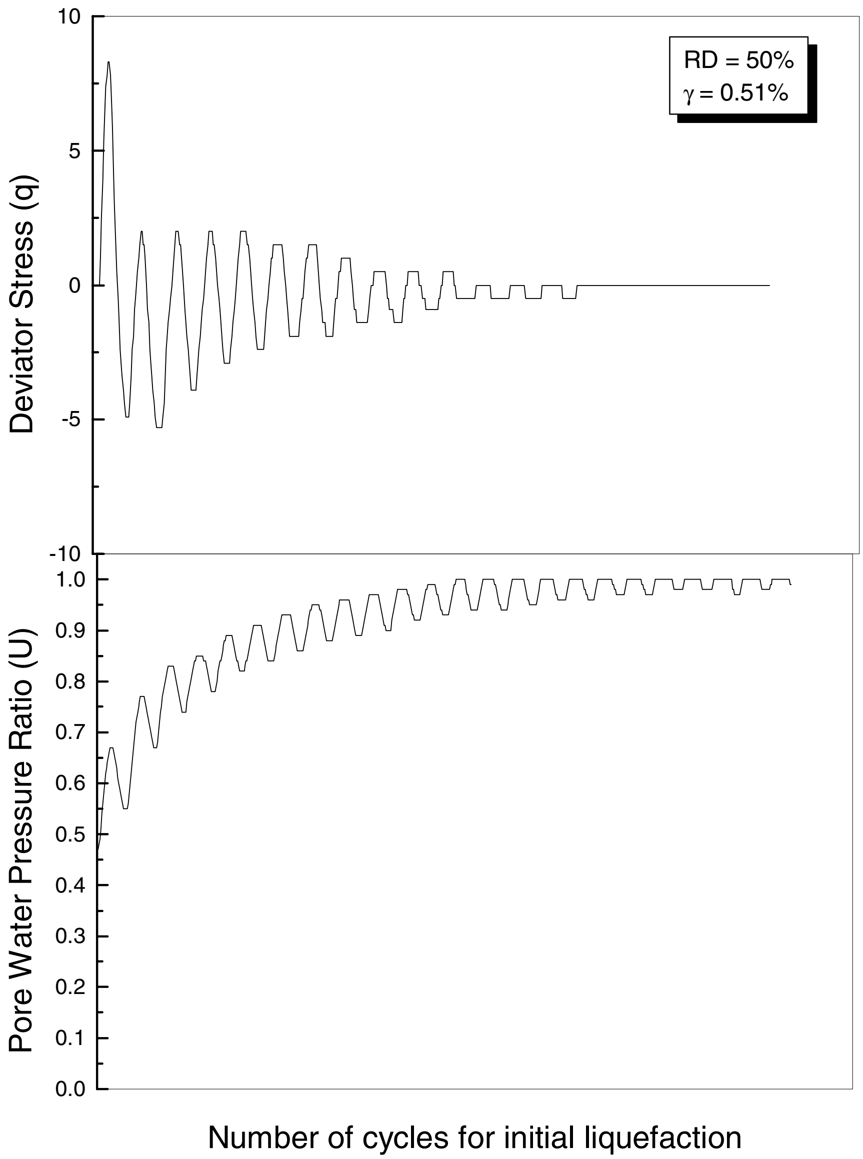

Fig.6 Variation of deviator stress and pore pressure ratio with number of cyclic shear strain

1 Associate Professor, Department of Civil Engineering, Indian Institute of Science, Bangalore (INDIA)
2 Research Scholars, Department of Civil Engineering, Indian Institute of Science, Bangalore (INDIA)
3 Professor, Department of Civil Engineering, Indian Institute of Science, Bangalore (INDIA)

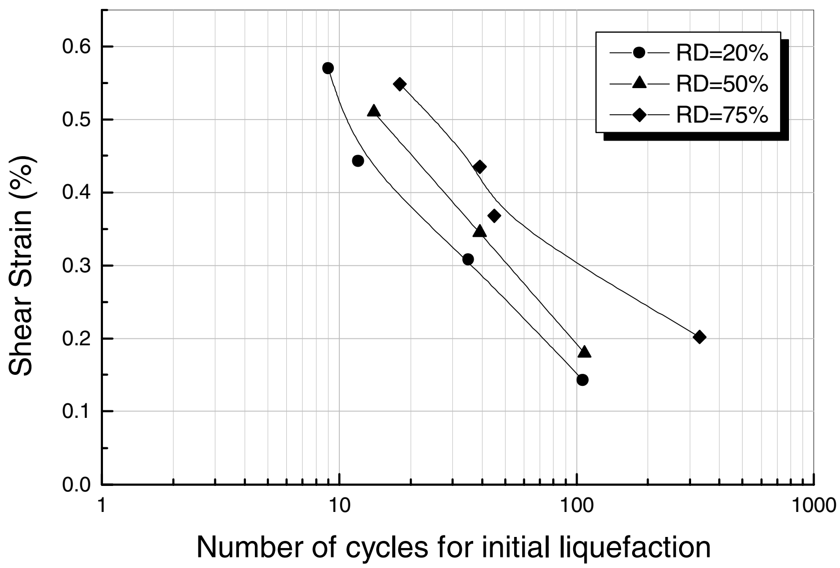

Fig.7 Liquefaction resistance curves for soil samples from Beltaghat

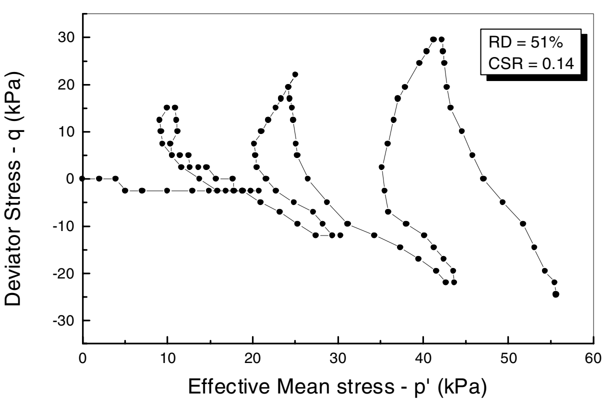

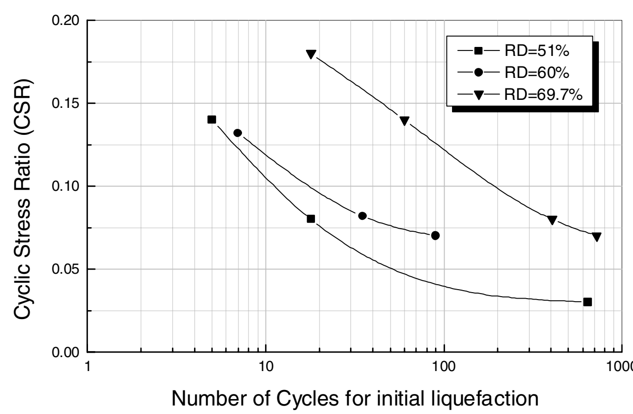

Fig. 8 Variation of mean stress with Deviator stress for Bhuj sample

Fig.9 Liquefaction resistance curves for soil samples from Bhuj

Undrained Monotonic Loading Tests

Undrained triaxial compression tests were carried out under monotonic loading condition in a strain-controlled manner with an axial strain rate of 0.6mm/minute on soil samples. Specimens prepared with a wide range of initial relative densities (RD_o) of 8.9%, 56.5% and 80% were isotropically consolidated to initial confining pressure ranging from 25 kPa to 450 kPa. The specimens were sheared to large strains to obtain steady state conditions. The steady state is achieved when the pore pressures become constant under continued shearing at large axial strains. The stress-strain, stress-path and stress ratio diagrams for a sample with relative density of 8.9% are presented in figures 10, 11 and 12 respectively. Here, the

1 Associate Professor, Department of Civil Engineering, Indian Institute of Science, Bangalore (INDIA)
2 Research Scholars, Department of Civil Engineering, Indian Institute of Science, Bangalore (INDIA)
3 Professor, Department of Civil Engineering, Indian Institute of Science, Bangalore (INDIA)

effective mean stress is defined by $p' = (\sigma'_1 + 2\sigma'_3) / 3$, while the deviator stress by $q = (\sigma'_1 - \sigma'_3)$ and e_c denotes the void ratio of the sample after isotropic consolidation

It is seen from the figure 11, that the effective confining stress at which the soil is consolidated has major implications in changing the behavior of silty sand from contractive to dilative. Silty sands in the range of void ratio 0.607 to 0.656 showing drastic reduction in strength at lower confining stress exhibit more and more dilative behavior at increasing confining stresses. This indicates that the silty sands become more stable at increasing confining stresses. This represents totally a different behavior when compared to the behavior of clean sands in loose state. It is just because clean sands normally exhibit the opposite trend of increase in stability with increasing confining pressures for initially loose states. Similar effects were reported by Yamamuro and Lade [3] by conducting undrained triaxial compression tests on Nevada sand with 7% fines content at an initial relative density of 30%.

Figures 13, 14 and 15 show the stress-strain, stress-path and stress ratio diagrams for the soil tested at relative densities of 56.5%. It is clear from Fig. 14 that, as the void ratio decreases (increase in density) silty sand exhibit more dilating behavior (25 to 50 kPa). This demonstrates the dependency of both void ratio and confining stress on the undrained behavior of silty sands. Only dilative behavior can be noticed from figure 17 in the range of void ratio 0.462 to 0.469 at a relative density of 80%.

Residual Strength

When relatively loose sand is strained in undrained shearing beyond the point of peak strength, the undrained strength drops to a value that is maintained constant over a large range in strain. This is conventionally called the undrained steady state strength or residual strength. However, if the strength increases after passing through a minimum value, the phenomenon is called limited or quasi-liquefaction. Even limited liquefaction may result in significant deformations and associated drop in strength. The residual strength S_{us} may be defined [2] as

$$S_{us} = (q_s /2) \cos\phi_s \tag{1}$$

where q_s and ϕ_s indicate the deviator stress and the mobilized angle of interparticle friction at the quasi-steady state. For the undrained tests carried out at various confining pressures and the initial state, the deviator stress (q_s) was estimated at quasi-steady state point along with a measurement of mobilized friction angle. Further as explained earlier, residual strength was estimated using equation (1). Figure 18 shows the evaluated residual strength and its variation with void ratio and confining stress. The residual strength decreases with increase in the void ratio of sample and further it increases with increasing effective confining pressure. Fig. 19 shows the normalized residual strength with void ratio. The preliminary results show a greater scatter and it may be attributed to the initial fabric of the sample.

1 Associate Professor, Department of Civil Engineering, Indian Institute of Science, Bangalore (INDIA)
2 Research Scholars, Department of Civil Engineering, Indian Institute of Science, Bangalore (INDIA)
3 Professor, Department of Civil Engineering, Indian Institute of Science, Bangalore (INDIA)

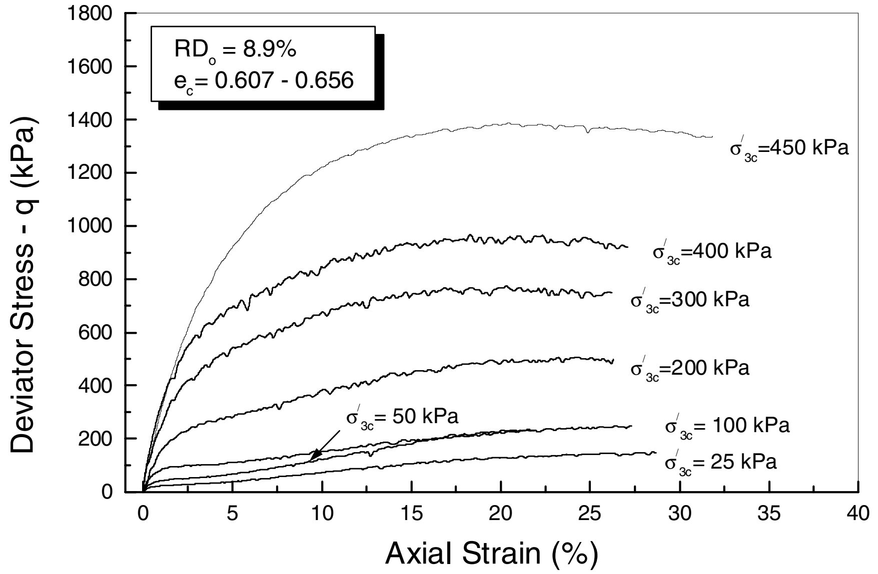

Fig.10 Stress-strain relationship

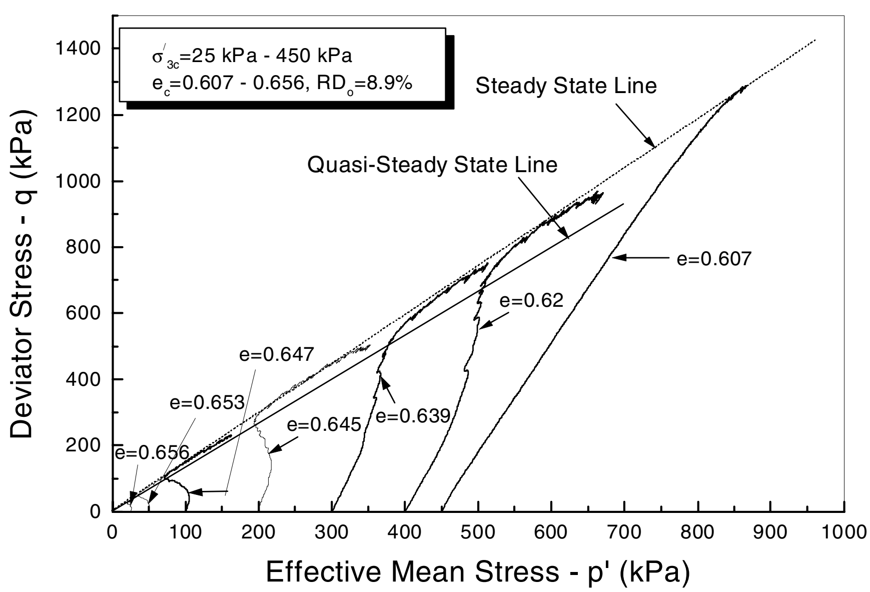

Fig.11 Stress path diagram

1 Associate Professor, Department of Civil Engineering, Indian Institute of Science, Bangalore (INDIA)
2 Research Scholars, Department of Civil Engineering, Indian Institute of Science, Bangalore (INDIA)
3 Professor, Department of Civil Engineering, Indian Institute of Science, Bangalore (INDIA)

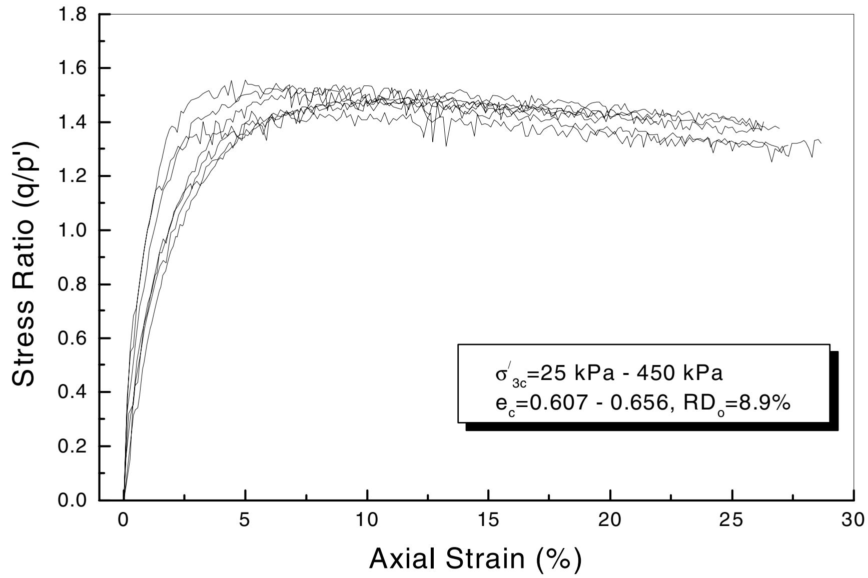

Fig.12 variation of stress ratio with axial strain

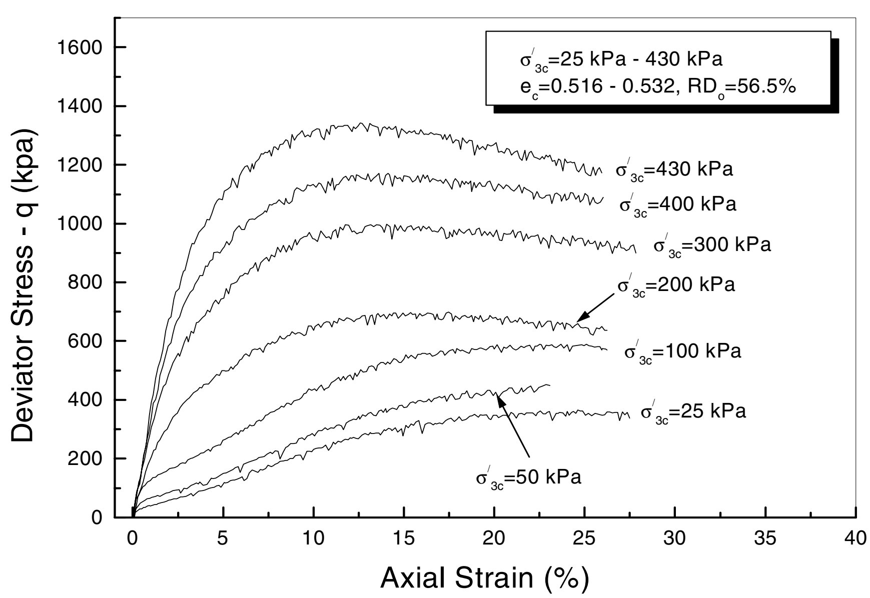

Fig.13 Stress-strain relationship

1 Associate Professor, Department of Civil Engineering, Indian Institute of Science, Bangalore (INDIA)
2 Research Scholars, Department of Civil Engineering, Indian Institute of Science, Bangalore (INDIA)
3 Professor, Department of Civil Engineering, Indian Institute of Science, Bangalore (INDIA)

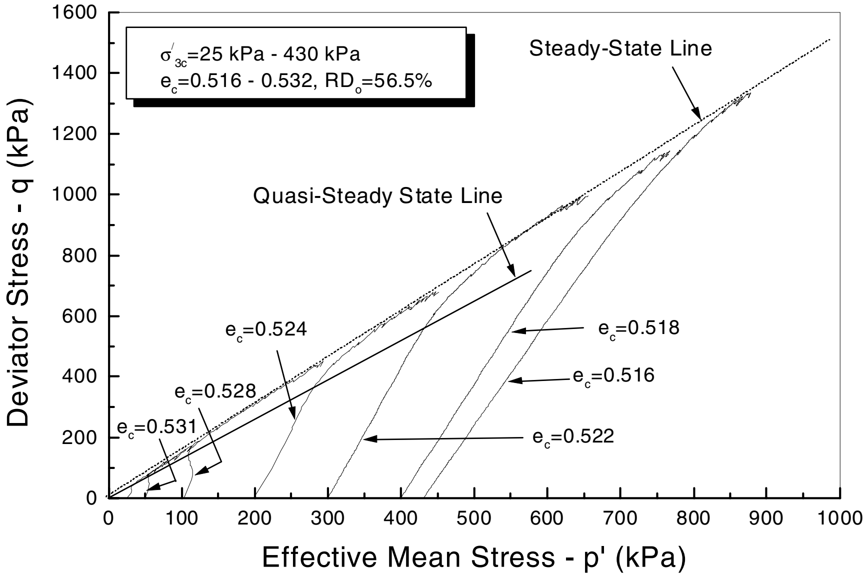

Fig.14 Stress path diagram

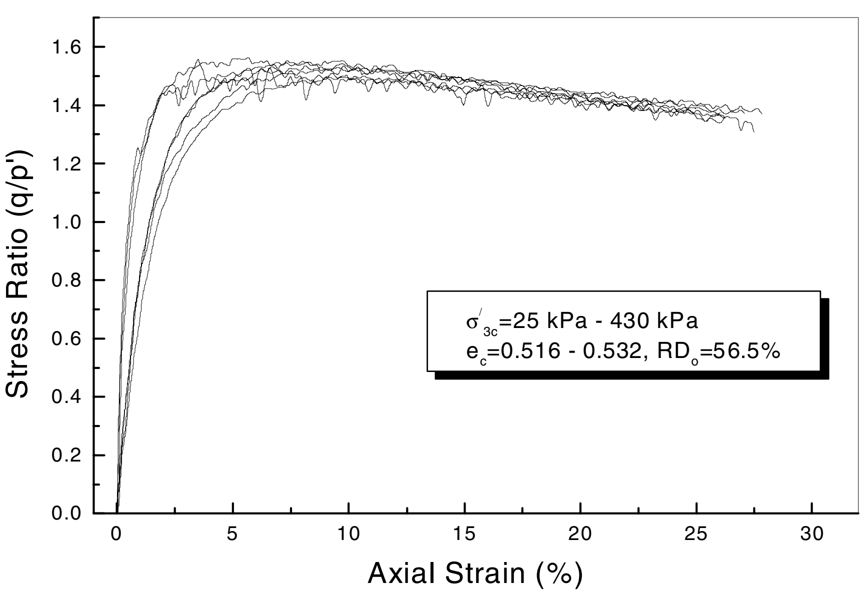

Fig.15 Variation of stress ratio with axial strain

1 Associate Professor, Department of Civil Engineering, Indian Institute of Science, Bangalore (INDIA)
2 Research Scholars, Department of Civil Engineering, Indian Institute of Science, Bangalore (INDIA)
3 Professor, Department of Civil Engineering, Indian Institute of Science, Bangalore (INDIA)

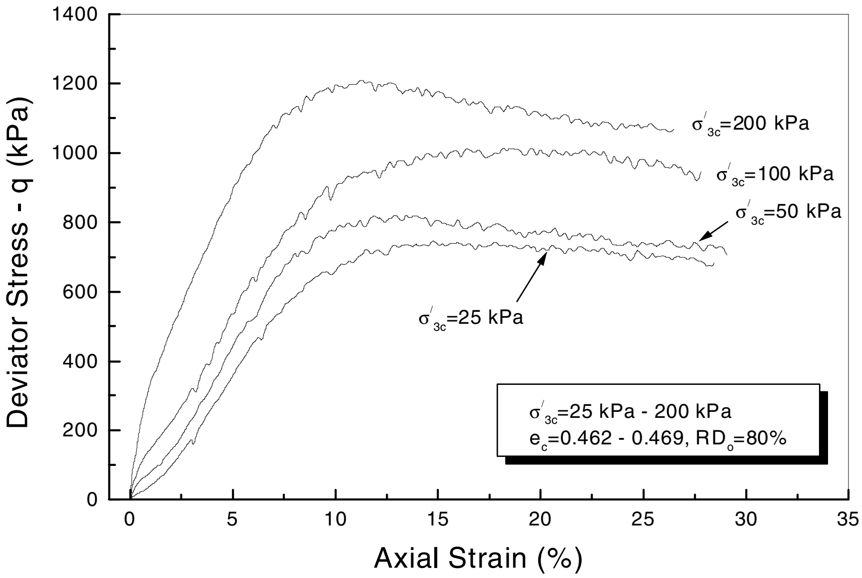

Fig.16 Stress strain diagram

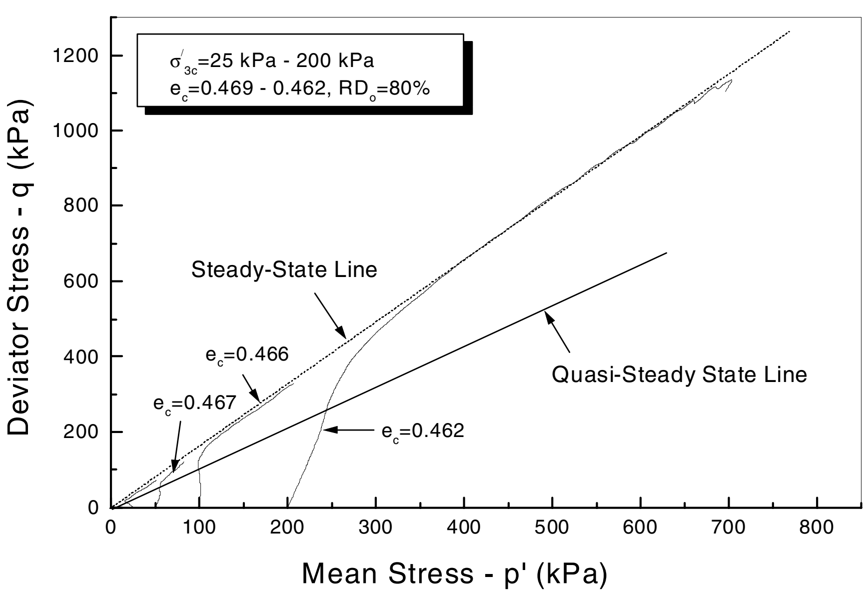

Fig.17 Stress path diagram

1 Associate Professor, Department of Civil Engineering, Indian Institute of Science, Bangalore (INDIA)
2 Research Scholars, Department of Civil Engineering, Indian Institute of Science, Bangalore (INDIA)
3 Professor, Department of Civil Engineering, Indian Institute of Science, Bangalore (INDIA)

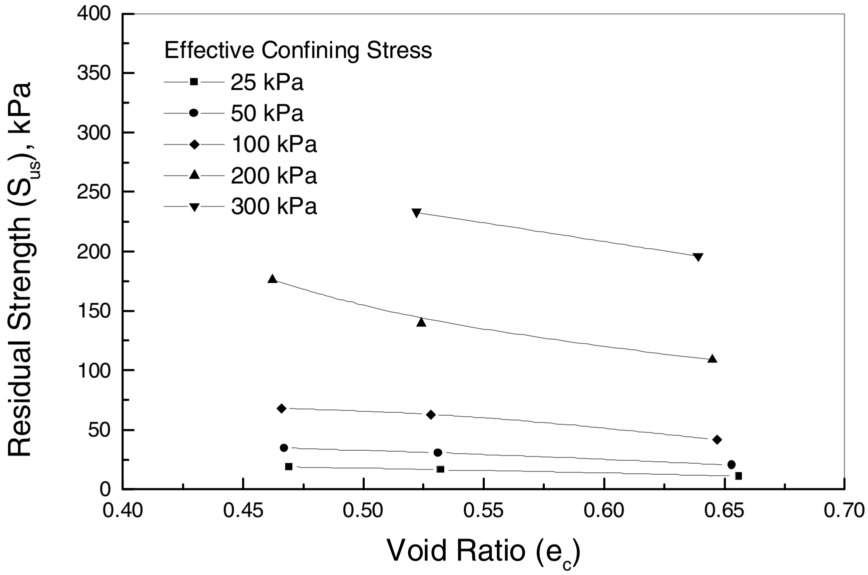

Fig.18 Variation of residual strength with void ratio and confining stress

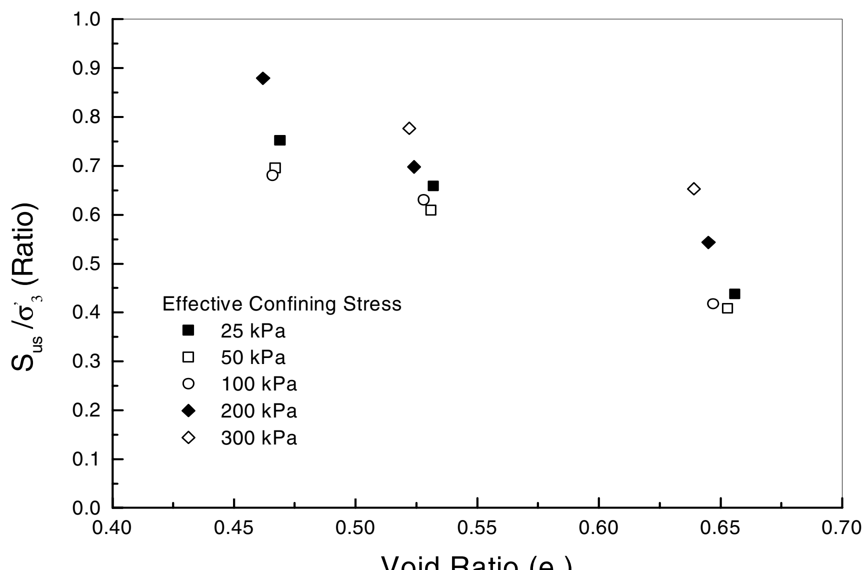

Fig. 19 Variation of normalized residual strength with void ratio

1 Associate Professor, Department of Civil Engineering, Indian Institute of Science, Bangalore (INDIA)
2 Research Scholars, Department of Civil Engineering, Indian Institute of Science, Bangalore (INDIA)
3 Professor, Department of Civil Engineering, Indian Institute of Science, Bangalore (INDIA)

CONCLUDING REMARKS

A series of undrained triaxial compression tests in cyclic and monotonic loading conditions were performed on liquefied silty sands from Beltaghat and Bhuj sites in India. As the magnitude of cyclic shear strain increases, the number of shear strain cycles required to initiate liquefaction reduces and thus indicating that the magnitude of shear strain govern the rate of pore pressure build up during cyclic loading. An increase in the relative density results an increase in the cyclic shear strain amplitude required to cause liquefaction. Stress-controlled cyclic tests results demonstrate that at higher cyclic stress ratios, the liquefaction occurs at lower number of cycles. An increase in the relative density results in an increase in the cyclic strength of the soil there by making it less susceptible to liquefaction at lower dynamic load amplitudes. Undrained monotonic shear tests performed on Bhuj sands (containing appreciable amounts of fines) with initial confining pressures between 25 kpa and 450 kPa showed contractive behavior at lower confining pressure than at higher values in the range of void ratios tested. Experimental data on silty sands indicate that the initial fabric might have a role along with void ratios and effective confining pressures on the residual strength.

ACKNOWLEDGMENT

The authors gratefully acknowledge the Department of Science & Technology, Government of India for financial support for the project " Insitu Evaluation of Soil Liquefaction Potential" under the grant No. DST/23/(287)/SU/2001.

REFERENCES

1. ASTM Designation: D 5311-92 (Reapproved 1996) “Standard Test Method for Load Controlled Cyclic Triaxial Strength of Soil”, Annual Book of ASTM standards, Vol. 04.08.

2. Ishihara K. “Liquefaction and flow failure during earthquakes”, Geotechnique, vol. 43,no. 3, pp. 351-415, 1993.

3. Yamamuro Jerry A. and Lade. Poul V. “Steady-state concepts and static liquefaction of siltysands”, Journal of Geotechnical and Geoenvironmental Engineering, vol. 124, no. 9, pp. 868-877, 1998.

4. Srivastav, S.K. "Bhuj earthquake of 26th January, 2001-some pertinent questions". Abstracts of International Conference on Seismic Hazard with particular reference to Bhuj Earthquake of January 26, 2001, 3-5 October, New Delhi, pp 3-5, 2001.

5. Sukhija B.S., Rao M.N, Reddy D.V, Nagabhushanam P, Hussain S, Chadha R.K. and Gupta H.K. “Paleoliquefaction evidence and periodicity of large prehistoric earthquakes in Shillong Plateau, India”, Earth and Planetary Science Letters, No.167, pp.269-282, 1999.

1 Associate Professor, Department of Civil Engineering, Indian Institute of Science, Bangalore (INDIA)
2 Research Scholars, Department of Civil Engineering, Indian Institute of Science, Bangalore (INDIA)
3 Professor, Department of Civil Engineering, Indian Institute of Science, Bangalore (INDIA)